# *In operando* studies of CO oxidation on epitaxial $SrCoO_{2.5+\delta}$ thin films

Chad M. Folkman, Seo Hyoung Chang, Hyoungjeen Jeen (iD), Edith Perret (iD), Peter M. Baldo, Carol Thompson, Jeffrey A. Eastman (iD), Ho Nyung Lee (iD), and Dillon D. Fong (iD)

View Online          Export Citation          CrossMark

## ARTICLES YOU MAY BE INTERESTED IN

# *In operando* studies of CO oxidation on epitaxial SrCoO$_{2.5+\delta}$ thin films

View Online      Export Citation      CrossMark

Chad M. Folkman,[1,a)] Seo Hyoung Chang,[1,2] Hyoungjeen Jeen,[3,4] (iD) Edith Perret,[1,5] (iD) Peter M. Baldo,[1]
Carol Thompson,[6] Jeffrey A. Eastman,[1] (iD) Ho Nyung Lee,[3] (iD) and Dillon D. Fong[1,b)] (iD)

## AFFILIATIONS

[1] Materials Science Division, Argonne National Laboratory, Argonne, Illinois 60439, USA
[2] Department of Physics, Chung-Ang University, Seoul 06974, South Korea
[3] Materials Science and Technology Division, Oak Ridge National Laboratory, Oak Ridge, Tennessee 37831, USA
[4] Department of Physics, Pusan National University, Busan 46241, Korea
[5] Laboratory for Advanced Fibers, Empa, Swiss Federal Laboratories for Materials Science and Technology,
Lerchenfeldstrasse 5, 9014 St. Gallen, Switzerland
[6] Department of Physics, Northern Illinois University, DeKalb, Illinois 60115, USA

a) Electronic mail: folkmanc@gmail.com
b) Electronic mail: fong@anl.gov

## ABSTRACT

The high abundance and fast kinetics of select transition metal oxide catalysts are attractive features for many chemical and electrochemical device applications. However, the activity of such catalysts can be accompanied by phase instabilities that prevent their widespread usage. Furthermore, complexities associated with variations in phase behavior and oxygen stoichiometry have hindered studies on the true origins of catalytic activity. Here, we explore the interactions between activity, phase stability, and microstructure using *in operando* synchrotron X-ray techniques and gas chromatography/mass spectroscopy (GCMS) to probe the behavior of model SrCoO$_{2.5+\delta}$ (SCO) catalysts. Pulsed laser deposition was used to prepare SCO thin films on (001) SrTiO$_3$, (111) SrTiO$_3$, and pseudocubic (001) DyScO$_3$ substrates. The GCMS catalytic measurements were performed with a custom-built microreactor compatible with a synchrotron X-ray diffractometer at the Advanced Photon Source. The activity for carbon monoxide oxidation was determined as a function of temperature from 500 °C to 800 °C. We show that the SrCoO$_{2.5+\delta}$ films are active for CO oxidation, most likely by direct reaction with lattice oxygen; consequently, the activity was observed to increase as the films become less stable, with the most active film being the one exhibiting the lowest surface and crystal quality. All films decompose at high temperatures, with *in operando* diffraction indicating the gradual formation of Sr-rich hexagonal and CoO phases. We find that real-time studies of model oxide systems with synchrotron X-rays is a powerful means of gaining insight into the varied processes taking place at catalytic surfaces.

Perovskite-type oxides have long been of interest as catalysts for a variety of chemical processes, including those relating to the oxygen evolution or reduction reaction.[1–7] From past work, it is known that an important criterion for high catalytic activity is optimal electron filling of the $e_g$ orbital. Accordingly, cobalt cations in the $3d^4$–$3d^6$ configuration typically exhibit high activities when incorporated within perovskite frameworks such as Ba$_{0.5}$Sr$_{0.5}$Co$_{0.8}$Fe$_{0.2}$O$_{3-\delta}$ or La$_{1-x}$Ca$_x$CoO$_{3-\delta}$.[8–12]

One of the chief advantages of the perovskite ABO$_3$ framework is its chemical flexibility, and catalytic properties can be tuned through judicious selection and mixing of the A- and B-cations.[3] Given the complexities associated with molecular adsorption on perovskite surfaces, defect formation, and structural destabilization, researchers are now exploring advances in machine learning for both accelerated screening of potential catalysts and identifying key descriptors for different reactions.[3,13] However, much remains to be

understood regarding the physical mechanisms that take place on both ideal and defective perovskite surfaces.

One of the primary challenges is determining and isolating the different contributions to catalytic activity. Perovskites are often electrical insulators, preventing most electrochemical measurements, and grain boundaries, impurities, and other defects associated with bulk samples can cause large differences in the measured gas-phase catalytic activity depending on how the material is prepared. Single-crystal surfaces would provide a simpler case study, but many bulk perovskite crystals cannot be grown, and the reduction in surface area from a powder to a single-crystal surface can be on the order of $10^6\times$ or more. This implies that measurement of the reaction products from single-crystal catalysts requires extreme sensitivity and that conventional packed bed or catalytic wall reactors[14] cannot be employed. In the traditional surface science approach to heterogeneous catalysis, gases are introduced to a single-crystal surface in high vacuum, and the surface is studied with vacuum-based techniques such as electron diffraction.[15] However, simple extrapolation of these results, especially those concerning the structure and chemistry of the active surface, to the high pressure/temperature conditions of industrial catalysts cannot easily be justified.[16] This has led to a discussion of both a "materials gap" (dealing with high vs low surface area materials) and a "pressure gap" (dealing with high pressure vs low pressure studies) when it comes to studies of heterogeneous catalysis.[17,18] Both must be bridged if we are to understand the inner workings of the catalytic process.

Here, we describe an *in operando* study of active perovskite surfaces as they undergo the model CO oxidation reaction. We utilize a microreactor custom built to mount onto a six-circle diffractometer at the Advanced Photon Source such that surface X-ray diffraction (SXRD) measurements can be conducted during the catalytic process (Ref. [19]). The catalyst of choice is $SrCoO_{2.5}$, an oxide that is similar to a perovskite but in which one out of every six oxygen ions is removed and ordered to form the oxygen-deficient brownmillerite structure (BM-SCO). The BM-SCO thin films were deposited by pulsed laser deposition (PLD) onto single crystal $SrTiO_3$ (001), (111), and $DyScO_3$ $(001)_p$ (pseudocubic) substrates.[20,21] Details of the deposition conditions are provided elsewhere.[22] In an earlier study, we demonstrated that epitaxial $SrCoO_{2.5}$ is indeed active for the CO oxidation reaction at elevated pressures and temperatures.[23]

A schematic of the microreactor cross section is shown in Fig. 1(a). The mechanical interface between the microreactor and diffractometer and the scattering geometry used to calculate reciprocal space coordinates are described elsewhere.[19,24] Important for the work presented here are the sample motions $Z$ and $\chi$, which are decoupled from the microreactor through the use of polytetrafluoroethylene rotary seals. The $Z$-motion is required for sample height adjustment at each temperature step, while the $\chi$-rotation around the sample normal is necessary for maintaining the Bragg condition in off-specular diffraction geometries. In this study, we employed 21 keV X-rays from an undulator source focused at the sample location to a vertical height of 30 $\mu$m (for grazing-angle studies) and a horizontal width of 3 mm. The flow rate of the inlet gas was set with mass flow controllers, and the outlet gas was sent to a commercial gas chromatography/mass spectrometry (GCMS) unit (Perkin Elmer Clarus 680) via a 20 $\mu$l sample loop [Fig. 1(b)]. Gas
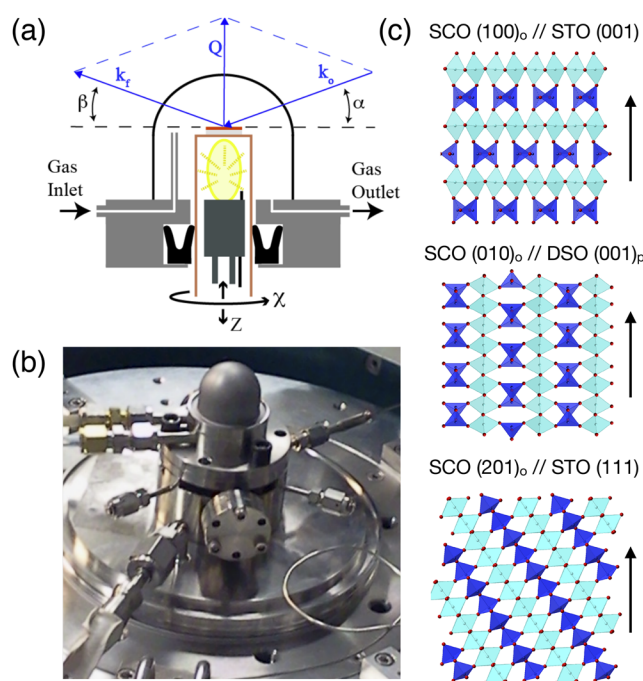


**FIG. 1**. Description of the *in operando* apparatus and materials systems. (a) Schematic of the microreactor allowing both catalytic studies and X-ray diffraction measurements. The sample is mounted atop a quartz tube affixed to both rotational and translational motors. We depict a symmetrical scattering geometry with incoming and outgoing wavevectors **k** and scattering vector **Q**, but off-specular geometries can also be employed. The gas flow direction is indicated. (b) Image of the Be-domed microreactor as mounted on a six-circle diffractometer. Lines for water cooling and gas handling are visible. (c) Cross-sectional views of the $SrCoO_{2.5}$ crystal structure for SCO films grown on STO (001) (top), DSO $(001)_p$ (middle), and STO (111) (bottom) substrates. Oxygen octahedra are colored light blue, and oxygen tetrahedra are colored dark blue. The arrows indicate the direction along the surface normal.

mixtures of 300 ppm $O_2$/He and 300 ppm CO/He were flowed continuously at 7 SCCM each through the reactor for a total flow rate of 14 SCCM. The total reactor pressure was fixed at 1.13 bars. We therefore run a steady-state flow reactor with low flow rates and small volumes rather than a batch-style reactor, in which the gas composition changes continually.[18,25]

It should be noted that the materials comprising the microreactor were chosen to minimize contributions of the reactor itself to the CO oxidation reaction. The halogen bulb heater is encased within a fused quartz tube (19 mm diameter) with a top plate for sample mounting. Hence, the heater environment, including the heating element leads, thermocouple, and fittings, is physically isolated from the microreactor volume. The dome material, composed of beryllium for optimal X-ray transmission, is brazed to a water-cooled stainless steel flange with Viton® seals [Fig. 1(b)]. The total volume of the reactor is 30 ml. The background activity level was determined by conducting measurements under conditions identical to those for the catalytic studies but without the BM-SCO film (with the perovskite substrate, however).

In bulk form, the BM-SCO crystal is orthorhombic (space group $Ima2$) with $a$ = 1.5745 nm, $b$ = 0.5574 nm, and $c$ = 0.5472 nm at room temperature.[26] Along the $a$-axis, the coordination polyhedra for the Co cation alternate between tetrahedra and octahedra. Its pseudotetragonal lattice parameters are $a_p = b_p = 0.3905$ nm and $c_p = 0.3936$ nm, with $c_p$ along the direction of alternating polyhedra. The $SrTiO_3$ (STO) substrate is cubic, with a lattice parameter of $a$ = 0.3905 nm, while the $DyScO_3$ (DSO) substrate is orthorhombic,[27] with a pseudocubic lattice parameter of $a_p = 0.395$ nm[21] (all at room temperature). Thus, while both substrates can induce epitaxial crystal growth,[23] BM-SCO is nearly unstrained on STO (with $c_p$ along the out-of-plane direction) and in slight biaxial tension on DSO (with $c_p$ along either of the in-plane directions). As a result, the tetrahedral and octahedral planes alternate along the out-of-plane direction on (001) STO and alternate along in-plane directions on $(001)_p$ DSO, as depicted in Fig. 1(c). These orientations were confirmed experimentally with X-ray diffraction.

Interestingly, the BM-SCO film grown on (111) STO exhibits primarily the $(201)_o$ surface orientation. In this geometry, the tetrahedral and octahedral layering direction is tilted ~35° with respect to the surface normal of the substrate, as shown in Fig. 1(c). Unlike the smooth 20 nm and 23-nm-thick films deposited on the (001) STO and $(001)_p$ DSO substrates, respectively, the 40-nm-thick $(201)_o$-BM-SCO film surface is rough, as will be discussed later. Also note that there are different orthorhombic domains in these films, but their effects are minor for the purposes of our discussion and are ignored here.

The activity data for the CO oxidation reaction are shown in Fig. 2 as a function of temperature during the *in operando* experiment. The CO oxidation reaction is

$$O_2 + 2CO \rightarrow 2CO_2. \qquad (1)$$

At elevated temperatures, the activity increases above the background level for the BM-SCO film catalysts. We also conducted measurements on a polycrystalline Pt thin film grown on $SrTiO_3$ (001), which exhibited activities more than a factor of 10 greater than the values shown here. The $SrCoO_x$ films are therefore relatively inactive compared to Pt but more active than the $SrTiO_3$ substrates.

*In operando* X-ray measurements were conducted along the specular rod, with the SCO/STO (001) and SCO/DSO $(001)_p$ results shown in Figs. 3(a) and 3(b), respectively. Generally, at ~600 °C and below, the films remain single crystalline. Above ~650 °C, other Bragg peaks appear. The $L \approx 1.91$ peak at 800 °C in (b) is near the 004 reflection of bulk $Co_3O_4$ (at $L = 1.95$), and Bragg peaks from both CoO and the Sr-rich hexagonal phase ($Sr_6Co_5O_{15}$, referred to as H-SCO) gradually appear.[26,28] The decomposition reaction is

$$6SrCoO_{2.5} \rightarrow CoO_{1+x} + Sr_6Co_5O_{15-\delta}. \qquad (2)$$
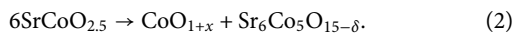
The activities in Fig. 2 confirm that CO oxidation takes place prior to decomposition of the brownmillerite structure. However, the activity could originate from oxygen within the BM-SCO film rather than from the flow of incoming $O_2$. In Fig. 4, we show the results of a separate grazing-angle measurement on $(100)_o$ $SrCoO_{2.5}$ conducted at the $\frac{1}{2}\frac{1}{2}\frac{5}{4}$ reflection (in terms of the reciprocal lattice units of the substrate) at 25 °C. The reason for such fractional indices
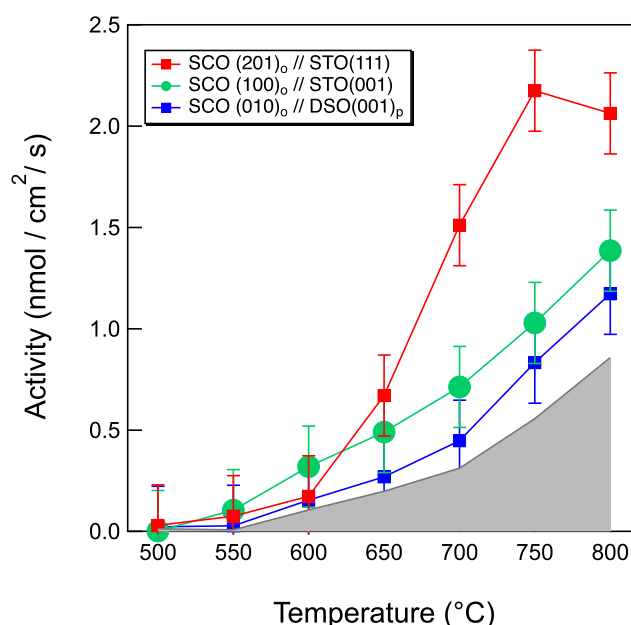


**FIG. 2**. Activity for $CO_2$ production as a function of temperature for the three differently oriented SCO films, as measured by gas chromatography/mass spectroscopy. The thicknesses are 40 nm for the SCO/STO(111), 20 nm for the SCO/STO(001), and 23 nm for the SCO/DSO(001)$_p$. The subscript "o" in the legend refers to the orthorhombic unit cell. The background level, as measured without the SCO film (but with the substrate), is shown by the gray-shaded area.

comes the orthorhombic unit cell of $SrCoO_{2.5}$, and the fact that it is larger than that of the substrate unit cell; in reciprocal space, this gives rise to reflections with fractional indices. As compared to integer reflections, the intensity of the $\frac{1}{2}\frac{1}{2}\frac{5}{4}$ contains a larger scattering contribution from the oxygen ions. The intensity also stems from only the $SrCoO_{2.5}$ film and not the substrate. The results suggest that (1) CO removes oxygen ions from the $SrCoO_x$ lattice, and (2) $O_2$ molecules dissociate on $SrCoO_x$, allowing oxygen ions to re-enter the lattice even at room temperature. Therefore, $O_2$ can evolve from the SCO lattice at low temperatures, and the production of $CO_2$ stems from the Mars-van Krevelen mechanism,[8,29] where CO reacts directly with lattice oxygen. This is in agreement with the conclusions of Jung *et al.*,[8] who studied the catalytic properties of $Nd_{1-x}Sr_xCoO_{3-y}$ powder catalysts as a function of $x$. They found that carbon monoxide oxidation occurs by direct reaction between the adsorbed carbon monoxide molecules and lattice oxygens. Vacancies at the surface serve as active sites for oxygen dissociation.

The $(201)_o$ BM-SCO film grown on (111) $SrTiO_3$ already exhibits a weak reflection from the H-SCO phase at 450 °C, as shown in Fig. 3(c). Based on the results of atomic force microscopy, we determine a root-mean-squared roughness value of 7.8 nm for this film, while the others grown on (001) substrates have a roughnesses of ~0.8 nm [Figs. 5(a)–5(c)]. It is presumed that layer-by-layer epitaxial growth of $SrCoO_x$ does not occur on $SrTiO_3$ (111), leading to a rough surface morphology. At 700 °C and above, the activity of
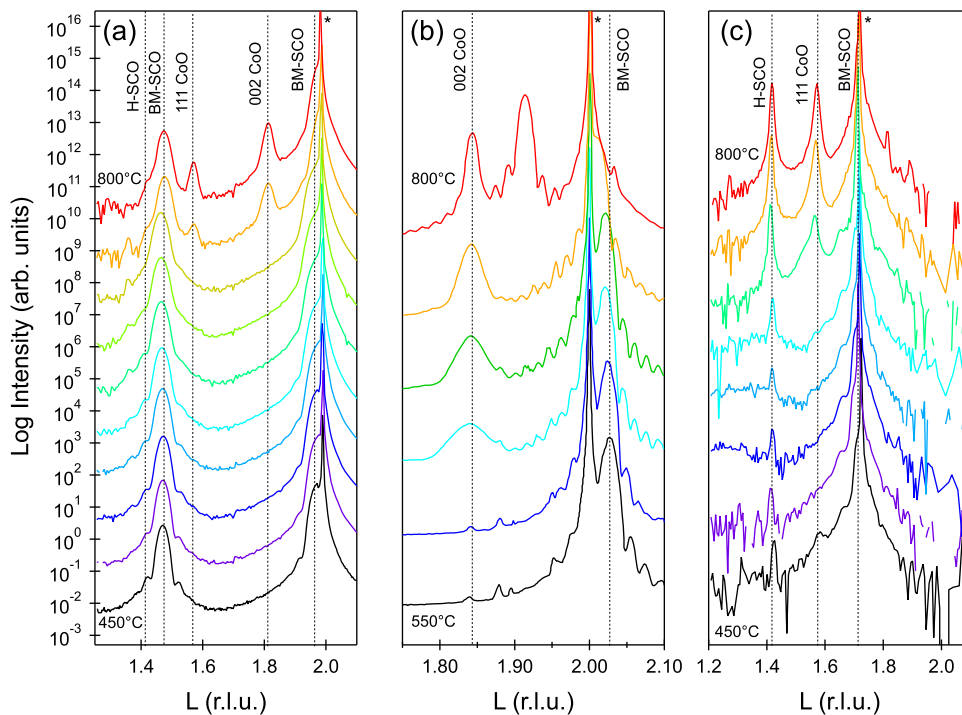
**FIG. 3**. *In operando* scattered X-ray intensities along the specular rod for (a) SCO/STO (001), (b) SCO/DSO $(001)_p$, and (c) SCO/STO (111) at different temperatures. The spectra are offset for clarity. The horizontal axis is referenced to reciprocal lattice units (r.l.u.) of the substrates, using the STO and DSO room temperature lattice parameters given above. The measurements were conducted in flowing CO and $O_2$ (0.17 mbar, each) while heating in 50 °C steps, from the lowest temperature (black) to the highest temperature (red). The known Bragg reflections are indexed, with * signifying the Bragg peak from the substrate. The reflection at $L \approx 1.91$ in (b) is near the bulk $Co_3O_4$ 004 (at $L = 1.95$).

the $(201)_o$-SCO film is more than twice that of the others (Fig. 2). It can also be observed from the diffraction results in Fig. 3 that portions of all three films have decomposed into H-SCO and CoO. This decomposition is clearly seen in the scanning electron micrographs presented in Figs. 5(d)–5(f), which show the postreaction structures.

To rationalize why SCO/STO (111) shows greater activity than the other films at 700 °C and above, we point to the specular rod scans in Fig. 3(c) and specifically the SCO Bragg peaks. While decomposition takes place in all of the films, it is evident that the SCO 402 reflection at $L \sim 1.7$ is absent at these temperatures. In the Mars-van Krevelen mechanism, CO removes oxygen directly from the lattice: this was already observed in the room temperature measurement of Fig. 4. The disappearance of the 402 reflection and the higher activity at ≥700 °C show that the accelerated removal of oxygen by CO leads to a collapse of the brownmillerite crystal structure. The process is presumably more pronounced for SCO/STO (111) because the initial film had the lowest overall surface and crystal quality. Although decomposition takes place for the SCO/DSO $(001)_p$ film, thickness fringes are still visible at 800 °C, indicating that the interfaces remains smooth and the crystal structure intact. This is consistent with the lower activity exhibited by the SCO/DSO $(001)_p$ sample (Fig. 2). The inverse relationship between activity and stability previously seen for SrRuO$_3$ of different crystal orientations[2] is also observed here.

In summary, we have conducted *in operando* synchrotron X-ray studies on thin film heterostructures of brownmillerite SrCoO$_{2.5}$. Using a custom-built, Be-domed microreactor, the catalytic activity of the CO oxidation reaction was measured as a function of temperature up to 800 °C. It was determined that all of

the SrCoO$_{2.5}$ films were active for CO oxidation, most likely by direct reaction with lattice oxygen. The activity was also shown to depend on crystal quality, with the lowest quality film in terms of surface roughness and crystallinity exhibiting the highest activity.
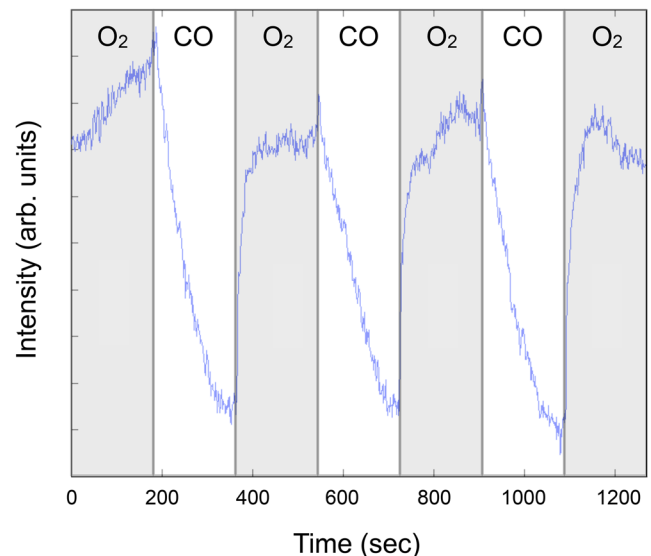


**FIG. 4**. X-ray results on the kinetic effects of gas injection. Integrated intensity of the $\frac{1}{2}\frac{1}{2}\frac{5}{4}$ reflection of BM-SCO $(100)_o$ is shown as a function of time as the environment is altered between 0.13 mbar $O_2$ and 267 mbar CO at room temperature. The measurements were conducted at an incidence angle of 0.1°.
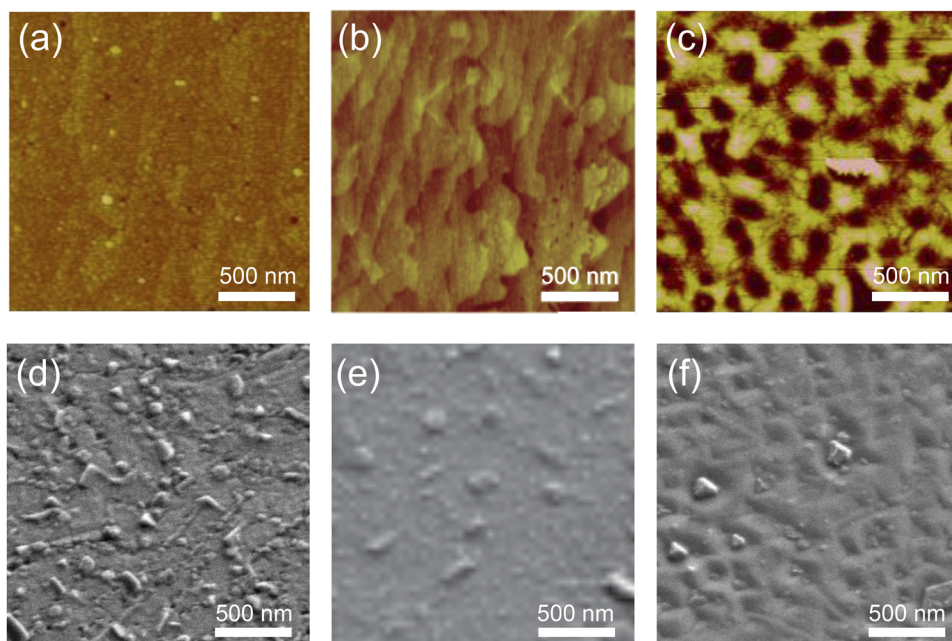
**FIG. 5**. As-grown and postreaction images taken at room temperature for the three differently oriented SCO films. Atomic force microscopy images are shown for the (a) as-grown SCO/STO (001), (b) as-grown SCO/DSO (001)$_p$, and (c) as-grown SCO/STO (111) films. Postreaction images (after the 800 °C temperature step) taken by scanning electron microscopy are shown in (d)–(f) according to the same sequence. Energy dispersive X-ray spectroscopy was used to investigate the composition of the protruding particles, finding them to be Co-rich.

All of the films decompose at high temperatures, and the diffraction results indicate the gradual formation of Sr-rich hexagonal and CoO phases.

As noted above, there is currently both a materials gap and a pressure gap when it comes to studies of heterogeneous catalysis. We have shown that when it comes to oxide materials, there may be an additional materials issue regarding activity and stability if the reactions involve the removal of lattice oxygen ions, as seen here. Reactive oxides with optimal $e_g$ orbital filling may be more susceptible to decomposition at elevated temperatures, and in this regard, many further studies are necessary. We find that studying the catalytic behavior of model systems, combining real-time synchrotron X-ray techniques with GCMS, is a powerful means of probing the origins of chemical activity and a promising avenue for elucidating the connections between structure, reactivity, and stability.

## REFERENCES

[1] S. Royer, D. Duprez, F. Can, X. Courtois, C. Batiot-Dupeyrat, S. Laassiri, and H. Alamdari, Chem. Rev. **114**, 10292 (2014).

[2] S. H. Chang, N. Danilovic, K. C. Chang, R. Subbaraman, A. P. Paulikas, D. D. Fong, M. J. Highland, P. M. Baldo, V. R. Stamenković, J. W. Freeland, J. A. Eastman, and N. M. Marković, Nat. Commun. **5**, 4191 (2014).

[3] J. Hwang, R. R. Rao, L. Giordano, Y. Katayama, Y. Yu, and Y. Shao-Horn, Science **358**, 751 (2017).

[4] F. Gunkel, L. Jin, D. N. Mueller, C. Hausner, D. S. Bick, C.-L. Jia, T. Schneller, I. Valov, R. Waser, and R. Dittmann, ACS Catal. **7**, 7029 (2017).

[5] J. H. Montoya, A. D. Doyle, J. K. Nørskov, and A. Vojvodic, Phys. Chem. Chem. Phys. **20**, 3813 (2018).

[6] Y. Wang, J. Li, and Z. Wei, J. Mater. Chem. A **6**, 8194 (2018).

[7] W.-J. Yin, B. Weng, J. Ge, Q. Sun, Z. Li, and Y. Yan, Energy Environ. Sci. **12**, 442 (2019).

[8] H. J. Jung, J.-T. Lim, S. H. Lee, Y.-R. Kim, and J.-G. Choi, J. Phys. Chem. **100**, 10243 (1996).

[9] T. Vaz and A. V. Salker, Mater. Sci. Eng.: B **143**, 81 (2007).

[10] I. C. Man, H.-Y. Su, F. Calle-Vallejo, H. A. Hansen, J. I. Martínez, N. G. Inoglu, J. Kitchin, T. F. Jaramillo, J. K. Nørskov, and J. Rossmeisl, ChemCatChem **3**, 1159 (2011).

[11] J. Suntivich, K. J. May, H. A. Gasteiger, J. B. Goodenough, and Y. Shao-Horn, Science **334**, 1383 (2011).

[12] J. Suntivich, H. A. Gasteiger, N. Yabuuchi, H. Nakanishi, J. B. Goodenough, and Y. Shao-Horn, Nat. Chem. **3**, 546 (2011).

[13] J. R. Kitchin, Nat. Catal. **1**, 230 (2018).

[14] L. Kiwi-Minsker and A. Renken, Catal. Today **110**, 2 (2005).

[15] G. Ertl, Surf. Sci. **299**, 742 (1994).

[16] J. Frenken and I. Groot, *Operando Research in Heterogeneous Catalysis* (Springer, 2016).

[17] S. Ferrer, M. D. Ackermann, and E. Lundgren, MRS Bull. **32**, 1010 (2007).

[18] R. van Rijn, M. D. Ackermann, O. Balmes, A. Dufrane, A. Geluk, H. Gonzalez, H. Isern, E. de Kuyper, L. Petit, V. A. Sole, D. Wermeille, R. Felici, and J. W. M. Frenken, Rev. Sci. Instrum. **81**, 014101 (2010).

[19] C. M. Folkman, M. J. Highland, E. Perret, S. K. Kim, T. T. Fister, H. Zhou, P. M. Baldo, S. Seifert, J. A. Eastman, P. H. Fuoss, and D. D. Fong, Rev. Sci. Instrum. **84**, 025111 (2013).

[20] A. Biswas, P. B. Rossen, C. H. Yang, W. Siemons, M. H. Jung, I. K. Yang, R. Ramesh, and Y. H. Jeong, Appl. Phys. Lett. **98**, 051904 (2011).

[21] J. E. Kleibeuker, B. Kuiper, S. Harkema, D. H. A. Blank, G. Koster, G. Rijnders, P. Tinnemans, E. Vlieg, P. B. Rossen, W. Siemons, G. Portale, J. Ravichandran, J. M. Szepieniec, and R. Ramesh, Phys. Rev. B **85**, 165413 (2012).

[22] H. Jeen, W. S. Choi, J. W. Freeland, H. Ohta, C. U. Jung, and H. N. Lee, Adv. Mater. **25**, 3651 (2013).

[23]H. Jeen, W. S. Choi, M. D. Biegalski, C. M. Folkman, I.-C. Tung, D. D. Fong, J. W. Freeland, D. Shin, H. Ohta, M. F. Chisholm, and H. N. Lee, Nat. Mater. **12**, 1057 (2013).

[24]T. T. Fister, P. H. Fuoss, D. D. Fong, J. A. Eastman, C. M. Folkman, S. O. Hruszkewycz, M. J. Highland, H. Zhou, and P. Fenter, J. Appl. Crystallogr. **46**, 639 (2013).

[25]P. Bernard, K. Peters, J. Alvarez, and S. Ferrer, Rev. Sci. Instrum. **70**, 1478 (1999).

[26]C. de la Calle, A. Aguadero, J. A. Alonso, and M. T. Fernández-Díaz, Solid State Sci. **10**, 1924 (2008).

[27]M. D. Biegalski, J. H. Haeni, S. Trolier-McKinstry, D. G. Schlom, C. D. Brandle, and A. J. V. Graitis, J. Mater. Res. **20**, 952 (2005).

[28]W. T. A. Harrison, S. L. Hegwood, and A. J. Jacobson, J. Chem. Soc., Chem. Commun. **14**, 1953 (1995).

[29]C. Doornkamp and V. Ponec, J. Mol. Catal. A: Chem. **162**, 19 (2000).